Asphalt Pavement Temperature Prediction

Manuel J. C. Minhoto* -- Jorge C. Pais -- Paulo A. A. Pereira****

**Instituto Politécnico de Bragança – Escola Superior de Tecnologia e de Gestão*
Campus de Santa Apolónia, Apartado 134, 5301-857 Bragança
minhoto@ipb.pt

*** University of Minho*
Department of Civil Engineering, Campus Azurém, 4800-058 Guimarães, Portugal
jpais@civil.uminho.pt
ppereira@civil.uminho.pt

ABSTRACT. *A 3-D finite element model (FEM) was developed to calculate the temperature of an asphalt rubber pavement located in the Northeast of Portugal. The goal of the case study presented in this paper is to show the good accuracy temperature prediction that can be obtained with this model when compared with the field pavement thermal condition obtained during a year. Input data to the model are the hourly values for solar radiation and temperature and the mean daily values of wind speed obtained from a meteorological station. The thermal response of a multilayered pavement structure is modelled using a FEM transient thermal analysis and each analysis was initiated with the full depth constant initial temperature obtained from field measurements. For each analysed day, the pavement temperature was measured at a new pavement section, located in IP4 main road, near Bragança, in the north of Portugal. At this location, seven thermocouples were installed in the asphalt rubber and conventional mix layers, at seven different depths. These pavement data was used to validate this simulation model, by comparing model calculated data with measured pavement temperatures. As conclusion, the 3-D finite-element analysis proved to be an interesting tool to simulate the transient behavior of asphalt pavements. The presented simulation model can predict the pavement temperature at different levels of bituminous layers with good accuracy.*

KEYWORDS: *asphalt rubber mix, temperature variation, thermal mixes behaviour, numerical analysis*

1. Introduction

Temperature variations have an important influence in the pavement thermal state. Depending on the temperature variation, stresses are induced in the overlay in two different ways, which need to be distinguished: through restrained shrinkage of the overlay and through the existing movements of slabs, due to the thermal shrinking phenomenon.

In order to calculate the pavement thermal effects and the asphalt concrete mix thermal response, it is necessary to evaluate the temperatures distribution at many depths of bituminous layers throughout typical twenty-four hours periods. The temperature distributions obtained for different hours, during the day, allow the calculation of thermal effects in the pavement, mainly in the overlay for rehabilitation studies.

The time variation of pavement thermal state is controlled by: climatic conditions, thermal diffusivity of the materials, thermal conductivity, specific heat, density and the depth below the surface (Sousa *et al.*, 2002).

The temperature distribution in a pavement structure can be obtained through field measurements, using temperature-recording equipment (Datalogger associated with thermocouples) or estimated by using mathematical models. The option of using the field measurement is desirable because actual temperature can be reliably measured and used in stress calculation models. However, this method is relatively slow and only provides information about temperatures in the observed period. On the other hand, a temperature theoretical model may suffer slightly due to lack of accuracies but will give a temperature distribution quickly and cheaply, and can be used to predict temperature distributions under a wide range of conditions, including any unusual or extreme conditions.

The simulation model proposed in this paper is based on Finite Element Method, involving weather data as input. The simulation model simulation was done by comparing the calculated temperatures with measured pavement temperatures, obtained in field since January 2004 until December 2004. The model computes the pavement temperatures by using measured climate data values as input.

Although this thermal approach may have a nature of a one-dimensional problem of the heat conduction in the vertical direction, given the infinite nature in the horizontal direction, the suggested model was developed in a three-dimensional basis, having in view its future compatibility with a 3-D mechanical reflective cracking model used by the authors in other projects.

The pavement temperatures prediction model is based on few basic principles. Once the hourly temperature distribution is governed by heat conduction principles within pavement and by energy interaction between the pavement and its surroundings, in the following chapter the main principles adopted in the proposed model are presented.

2. Thermal model

Conjugating the first law of the thermodynamics, which states that thermal energy is conserved, and Fourier's law, that relates the heat flux with the thermal gradient, the problem of heat transfer by conduction within the pavement is solved. For an isotropic medium and for constant thermal conductivity, this adopted principle is expressed as follows (Dewit, 1996 and Ozisik, 1985):

$$\nabla^2 T = \frac{1}{\alpha} \cdot \left(\frac{\partial T}{\partial t} \right) \quad [1]$$

where: $\nabla^2 = (\partial^2/\partial x^2) + (\partial^2/\partial y^2) + (\partial^2/\partial z^2)$

$\alpha = \dfrac{k}{\rho \cdot C}$ – Thermal diffusivity;

k – thermal conductivity;

ρ – density;

C – specific heat;

t – time.

On a sunny day the heat transfer by energy interaction between pavement and its surroundings consists of radiation balance and of exchanges by convection. The radiation balance (or thermal radiation) involves the consideration of outgoing longwave radiation, longwave counter radiation and the shortwave radiation (or solar radiation) (Hermansson, 2001).

The earth surface is assumed to emit longwave radiation as a black body. Thus, the outgoing longwave radiation follows the Stefan-Boltzman law (Dewit, 1996 and Hermansson, 2001):

$$q_e = \varepsilon_e \sigma T_s^4 \quad [2]$$

where: q_e – outgoing radiation;

ε_e – emission coefficient;

σ – Stefan-Boltzman constant;

T_s – pavement surface temperature.

As the atmosphere absorbs radiation and emits it as longwave radiation to the earth, this counter radiation absorbed by the pavement surface is calculated as proposed by (Dewit, 1996 and Hermansson, 2001):

$$q_a = \varepsilon_a \sigma T_{air}^4 \quad [3]$$

where: q_a – absorbed counter radiation;

ε_a – pavement surface absorptivity for longwave radiation and the amount of clouds;

T_{air} – air temperature.

Several authors (Donath *et at.*, 2002 and Picado-Santos L, 1994) consider the longwave radiation intensity balance (or thermal radiation) through the following expression:

$$q_r = h_r(T_{sur} - T_{air}) \quad [4]$$

where: q_r – longwave radiation intensity balance:
h_r – thermal radiation coefficient.

The expression used to obtain h_r is the following (Donath *et at.*, 2002):

$$h_r = \varepsilon\sigma(T_{sur} + T_{air})(T_{sur}^2 + T_{air}^2) \quad [5]$$

where: ε – emissivity of pavement surface.

Part of the high frequency (shortwave) radiation emitted by the sun is diffusely scattered in the atmosphere of the earth in all directions and the diffuse radiation that reach the earth is called diffused incident radiation. The radiation from the sun reaching the earth surface, without being reflected by clouds or absorbed or scattered by atmosphere, is called direct incident shortwave radiation. The total incident radiation (direct and diffused) can be estimated using the following equation (Dewit et al., 1996, Ozisik, 1985 and Donath et al., 2002):

$$q_i = \eta s_c f \cos\theta \quad [6]$$

where: q_i – thermal incident solar radiation;
η – loss factor accounting for scattering and absorption of shortwave radiation by atmosphere;
S_c – solar constant assumed to be 1353 W/m^2;
f – factor accounting the eccentricity of earth orbit;
θ – zenith angle.

The effective incident solar radiation absorbed by pavement surface may be determined by the equation (Hermansson, 2001):

$$q_s = \alpha_s \cdot q_i \quad [7]$$

where q_s – incident solar radiation absorbed by pavement surface;
α_s – solar radiation absorption coefficient.

In the model suggested in this paper, shortwave radiation is given as input data obtained from measured values.

The convection heat transfer between the pavement surface and the air immediately above is given as (Hermansson, 2001 and Donath et al., 2002):

$$q_c = h_c(T_{sur} - T_{air}) \quad [8]$$

where: q_c – convection heat transfer;
h_c – convection heat transfer coefficient.

The convection heat transfer coefficient can be calculated as proposed by (Hermansson, 2001 and Donath et al., 2002):

$$h_c = 698.24\left[\left(1.44\text{x}10^{-4}\,T_{ave}^{0.3}\,U^{0.7}\right)+\left(9.7\text{x}10^{-4}\,(T_{sur}-T_{air})^{0.3}\right)\right] \quad [9]$$

where: T_{ave} – average temperature given by $T_{ave} = (T_{sur} - T_{air})/2$;
U – wind speed.

3. Finite Element Method

This study is based on the use of the finite-element method in the prediction of temperature distributions in pavements. In the last years, this methodology has revealed to be a tool of great applicability in the pavements research domain. Thus, the theoretical basis of this methodology and the application for proposed simulation model, are described.

The first law of thermodynamics, which states that thermal energy is conserved, was used to build the solution of pavement thermal problem through finite elements. Considering a differential control volume of a pavement, in that methodology, the conservation of thermal energy is expressed by:

$$\rho C\frac{\partial T}{\partial t}+\{L\}^T\{q\}=0 \quad [10]$$

where: ρ – density;
C – specific heat;
T – temperature = T(x,y,z,t));
t – time;

$\{L\}=\begin{Bmatrix}\partial/\partial x\\ \partial/\partial y\\ \partial/\partial z\end{Bmatrix}$ - Vector operator;

$\{q\}$ – heat flux vector.

It should be noted that the term $\{L\}^T\{q\}$ may also be interpreted as $\nabla\{q\}$, where ∇ represents the divergence operator. Fourier's law can be used to relate the heat flux vector to the thermal gradients through the following expression:

$$\{q\}=-[D]\{L\}T \quad [11]$$

where: $[D]=\begin{bmatrix} K_{xx} & 0 & 0 \\ 0 & K_{yy} & 0 \\ 0 & 0 & k_{zz} \end{bmatrix}$ - conductivity matrix;

K_{xx}, K_{yy}, K_{zz} – thermal conductivity in the element x, y and z directions, respectively.

Expanding Equation [10] to its more familiar form:

$$\rho C\frac{\partial T}{\partial t}=\frac{\partial}{\partial x}\left(K_{xx}\frac{\partial T}{\partial x}\right)+\frac{\partial}{\partial x}\left(K_{yy}\frac{\partial T}{\partial y}\right)+\frac{\partial}{\partial x}\left(K_{zz}\frac{\partial T}{\partial z}\right) \quad [12]$$

Considering the isotropy of material ($K=Kxx=Kyy=Kzz$):

$$\rho C\frac{\partial T}{\partial t}=\frac{\partial}{\partial x}K\left\{\left(\frac{\partial T}{\partial x}\right)+\frac{\partial}{\partial x}\left(\frac{\partial T}{\partial y}\right)+\frac{\partial}{\partial x}\left(\frac{\partial T}{\partial z}\right)\right\} \quad [13]$$

Three types of boundary conditions, which cover the entire model, were considered: heat flow acting over the model surface limits; surface convection applied in the superior surface of model and the radiant energy between the model superior surface and its surroundings.

Specified heat flow acting over a surface follows the general expression:

$$\{q\}^T\{\eta\}=-q^* \quad [14]$$

where: $\{\eta\}$ – unit outward normal vector;
q^* – specified heat flow.

Specified convection surfaces heat flows acting over a surface follows the general expression:

$$\{q\}^T\{\eta\}=h_f\left(T_{sur}-T_{air}\right) \quad [15]$$

where h_f – convection coefficient;
T_{sur} – temperature at the surface of the model;
T_{air} – bulk temperature of the adjacent fluid.

Radiant energy exchange between a surface of the model and its surroundings is translated by the following expression, which gives the heat transfer rate between the surface and a point representing the surroundings:

$$q_r=\sigma\varepsilon\left(T_{sur}^4-T_{air}^4\right) \quad [16]$$

where σ – Stefan-Boltzman coefficient;
ε – effective emissivity;
q_r – heat flux loss of surface.

4. 3-D FEM Pavement thermal model

The 3-D Finite-Element Method was used for modelling the thermal behaviour of pavement. The pavement structures traditionally are idealized as a set of horizontal layers of constant thickness, homogeneous, continuous and infinite in the horizontal direction, resting on a subgrade, semi-infinite in the vertical direction. The thermal configuration of the pavement model was defined in basis of those principles and is presented in Figure 1. This model considers the possibility of thermal data transfer for a mechanical model with the same mesh.

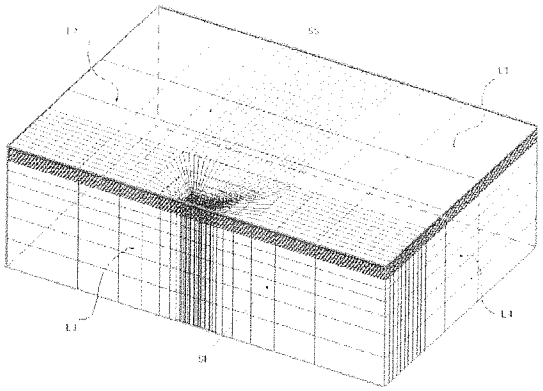

Figure 1. *Finite element mesh for thermal model*

The adopted mesh was designed also for study of the reflective cracking phenomenon due to the traffic loading and represents an existing pavement, where a crack is simulated through an element with zero-stiffness, and a layer on top of the existing pavement representing an overlay. This mesh was described in other works of the authors (Minhoto *et al.*, 2003 and Minhoto *et al.*, 2005).

The finite element model used in numerical thermal analysis was performed using a general finite elements analysis source code, ANSYS 7.0. This analysis is a 3-D transient analysis, using a standard finite element discretization, in space. In the design of the thermal finite-element mesh, the compatibility of mesh with other mechanical models was observed.

The designed mesh has 13538 elements. For three-dimensional thermal analysis, 3-D solid element, SOLID70, was used. This element, applicable to a three-dimensional transient thermal analysis, has capability for three-dimensional thermal

conduction, according with previous explanation. The element has eight nodes with a single degree of freedom, defined as temperature, at each node.

The thermal properties of pavement material, such as thermal conductivity, specific heat and density, for each pavement layer, were defined in the "material properties" of this element, when the model was developed.

For surface effect applications, such as radiation exchanges by convection heat transfer, the surface element SURF152 was used. The geometry, node locations, and the system coordinates for this element are shown in the Figure 2.

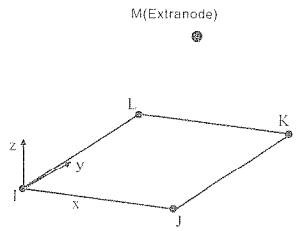

Figure 2. *3-D Surface Thermal element (SURF152)*

The element is defined by four nodes and by material properties. An extra node (away from the base element) is used for simulating the effects of convection and radiation and represents the point where the hourly air temperature is introduced as representative of the atmosphere. This element was overlaid onto an area face of 3-D thermal element SOLID70, located near top of model (pavement surface) as it shows in Figure 3.

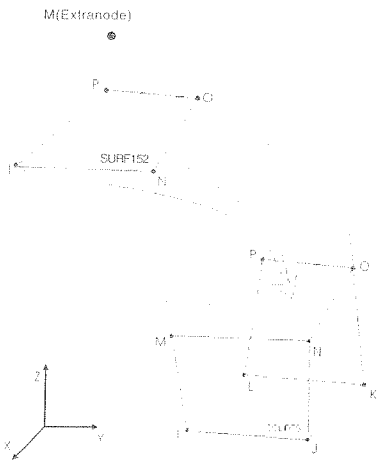

Figure 3. *SURF152 and SOLID70 coupling*

The element is applicable to three-dimensional thermal analysis and allows these load types and surface effects, such as heat fluxes, to exist simultaneously. The surface elements were placed on entire surface SS (Figure 1).

In the conductivity matrix calculation, for considering surface convection, the convection coefficient (or film coefficient) must be used. When extra node is used, its temperature becomes the air temperature. This element allows for radiation between the surface and the extra node "M". The emissivity of the surface is used in the conductivity matrix calculation, for considering surface radiation, and the Stefan-Boltzman constant is also used for the conductivity matrix calculation.

The solar radiation is considered as a heat flux that is applied on surface SS. In order to define the boundary conditions a null heat flux is applied on surfaces L1, L2, L3, L4 and SI, presented in the Figure 1.

5. Pavement Temperature prediction – case study

The main goal of this study is to show the good accuracy temperature prediction that can be obtained with the model presented in this paper when compared to the field pavement thermal condition in several representative days of the year.

Firstly, a FEM numerical analysis for the temperature distribution in a pavement of a trial section was performed for the weather conditions (air temperature, solar radiation and wind speed) obtained from January 2004 to December 2004 (Minhoto *et al.*, 2005). The model validation was made by statistical analysis between the FEM numerical temperature results and the field-measured temperatures and presented in Minhoto *et al.* (2005).

In this study, a set of thermal daily data was selected to perform a study about the accuracy of the temperature prediction that can be obtained with this model. This set of days was selected along the year and have typical daily air temperatures evolution, characterized by a combination of maximum and minimum temperature. The adopted values for the maximum temperatures were the following: 35ºC, 30ºC, 25ºC, 20ºC, 25ºC and 10ºC. The adopted values for minimum temperatures were: 20ºC, 15ºC, 10ºC, 5ºC, 0ºC and -5ºC. The combination of these two temperatures allowed to define 24 days which were studied in the work.

For each selected day, the thermal hourly data was used by the 3-D FEM model, as input data, and, as result, the hourly temperature in all nodes was computed. Then, the obtained value for nodes, that represents the pavement observed points, was compared with the measured field temperatures at those locations.

5.1. *Field data collection*

During a year (January 2004 to December 2004), pavement temperatures were measured at a newly pavement section, located at IP4 main road, near Bragança, in the northeast of Portugal. At that location, seven thermocouples were installed in the pavement layer, at seven different depths: at surface, 27.5 mm, 55 mm, 125 mm, 165 mm, 220 mm and 340 mm. The top one was installed just at the pavement surface. The depths for the other six were chosen to give a good representation of the whole asphalt layers. Pavement temperatures were recorded every hour, every day during the year.

With respect to short–term temperature response, it can be argued that subgrade temperature at 2.0 m depth is reasonably constant over a given months.

From a meteorological station, located near the test pavement section, it was obtained the hourly measurements of weather parameters, such as air temperature, solar radiation intensity and wind speed. These measurements were used as input data in the simulation models, to carry out temperature distribution prediction in a 340-mm full-depth pavement.

5.2. *Input data to simulation*

The pavement surface thermal emissivity for estimating the longwave radiation intensity balance was equal to 0.9 and the solar absorption coefficient was equal to 0.95. Table 1 presents the values for pavement material thermal properties adopted in this study. The parameters were adapted to give a good correspondence between calculated and measured pavement temperatures. The adopted values follow the typical values for those parameters suggested on bibliography by de Bondt (2000), A. Shalaby *et al.* (1990) and Hermansson (2001).

Table 1. *Layers Thermal Properties*

	Thickness (m)	K (W/°C.m)	C (W.s/kg.°C)	density (kg/m^3)
Overlay –asphalt rubber mix	0.055	1.5	850	2550
Overlay – conventional mix	0.070	1.5	860	2350
Cracked layer	0.215	1.5	850	2550
Sub-base	0.300	1.5	805	2370
subgrade	-	1.79	1100	2200

As expressed in the conclusions obtained from simulation made by Hermansson (2001), the influence of the thermal conductivity of the pavement is marginal for the pavement temperatures close to the surface. Thus, no further effort was made in this paper, to study the influence of thermal conductivity variation.

5.3. *Analysis procedure*

The thermal response of FEM simulation model, representing a multilayered pavement structure, was modelled using a transient thermal analysis for a several daily time-period, representing the selected representatives days. It is assumed that the pavement hourly temperature profile depends entirely on hourly air temperature value, hourly solar radiation value and wind speed daily mean value.

The analysis procedure involves a multiple 3-D finite-element runs and was initiated with the full depth at constant initial temperature, obtained from measured field temperatures. The analysis procedure was carried out for a periodicity of one hour.

5.4. *Results*

As a measure of error, the difference between calculated and measured pavement temperatures were calculated for every hour, for every depth and for each selected day. Also the average difference was determined for all pavement depths and for each computed situation of a selected day. Table 2 presents the result of this procedure and presents the average errors and the standard deviation of errors where one can conclude that the proposed model allowed to obtain excellent temperature prediction mainly in the top layers. The presence of an asphalt rubber mixture in the top of the pavement analysed did not affect the temperature prediction in the other pavement layers and depths.

Figures 4 to Figure 7 present the temperature evolution for four representative days (2nd March, 24th April, 24th July and 16th October), each one for each season of the year, and a comparison between the FEM calculated temperature and the in pavement measured temperature is made.

These figures allow to conclude that the temperature model used to predict the pavement temperature presents a good accuracy in the prediction of the temperature in the first layers of the pavement where the differences between calculated and observed temperatures are too small.

As the depth in the pavement increases, the model presents some problems in the prediction of the pavement temperature. For 0.340 m the temperature difference can reach 4 °C. Some important differences can also be found in surface for hot days, mainly in the summer, where 8 °C was found.

However, the presented model is an interesting tool to predict the pavement temperature until 0.30 m. The presence of an asphalt rubber mix layer in the top of the pavement did not affect the pavement temperature prediction.

Table 2. *Average errors and standard deviation in the temperature prediction*

		Air Temperature (ºC)		Temperature error (ºC)		Average erros at several pavement depths						
Day-Month	Season	maximum	minimum	average	s. deviation	0.00m	0.0275m	0.055m	0.125m	0.165m	0.220m	0.340m
21 Jan	Winter	10.6	-5.1	1.208	1.104	2.237	1.912	1.779	1.792	0.915	0.295	0.387
12 Feb	Winter	16.8	-3.7	0.155	1.149	1.402	1.711	0.830	0.517	0.861	0.276	0.483
2 Mar	Winter	9.3	-7.8	-0.673	1.800	1.041	1.137	0.776	1.391	1.836	1.874	2.779
31 Mar	Spring	10.5	5.2	0.444	1.059	1.372	1.229	0.903	0.314	0.553	0.256	1.152
14 Apr	Spring	15.2	-0.3	-2.515	3.050	3.440	3.267	3.300	3.687	3.607	2.337	3.999
23 Apr	Spring	18.8	-0.2	-2.324	2.613	3.017	2.518	2.831	3.170	3.309	2.123	3.936
24 Apr	Spring	22.7	2.1	-2.338	2.696	3.189	2.641	2.900	3.149	3.186	1.740	4.352
10 May	Spring	15.2	5.5	-1.261	1.547	0.983	1.276	1.115	1.992	2.447	2.433	1.901
22 May	Spring	19.7	10	-2.758	2.473	3.559	3.094	3.113	3.633	3.630	3.805	2.276
31 May	Spring	25.8	9.7	-2.925	2.800	4.308	3.301	3.541	3.468	3.541	2.904	3.856
4 Jun	Spring	29.4	9.6	-3.452	3.497	5.660	4.616	4.579	4.155	3.921	3.267	4.562
30 Jun	Summer	30.3	14.6	-2.846	3.386	5.029	4.121	3.984	3.500	3.353	2.614	4.163
9 Jul	Summer	20.7	5.8	-3.228	2.985	5.593	4.647	4.392	3.405	3.268	2.045	1.171
24 Jul	Summer	34.5	15.5	-3.156	2.849	4.623	3.762	3.877	3.622	3.763	2.756	4.497
26 Jul	Summer	32.1	12.8	-3.466	3.426	5.360	4.605	4.490	4.092	4.123	3.251	4.689
2 Ago	Summer	29	17.3	-1.806	3.035	3.348	2.790	2.583	2.578	2.577	2.215	4.095
4 Ago	Summer	25.2	14.8	-3.566	3.129	3.998	3.540	3.794	4.293	4.680	4.841	3.666
8 Ago	Summer	20.9	15.2	-0.427	2.627	1.738	1.785	1.199	1.391	1.377	1.891	5.102
26 Sep	Autumn	24.9	4.6	-2.845	1.896	2.906	2.451	2.506	3.046	3.485	3.670	3.342
29 Sep	Autumn	27.8	5.3	-1.498	1.635	2.841	2.011	2.019	1.584	1.784	0.952	0.584
16 Oct	Autumn	14.5	9.7	0.414	0.627	1.006	0.887	0.841	0.346	0.350	0.166	0.307
19 Nov	Autumn	5.6	-0.4	-0.743	0.811	1.425	1.222	0.951	0.719	0.783	0.656	0.791
20 Nov	Autumn	10.3	-0.3	-0.682	1.425	1.610	0.752	1.197	0.933	1.154	0.779	0.921
7 Dec	Autumn	4.3	-3.8	-0.722	0.628	0.757	0.539	0.639	0.908	1.113	1.013	0.699

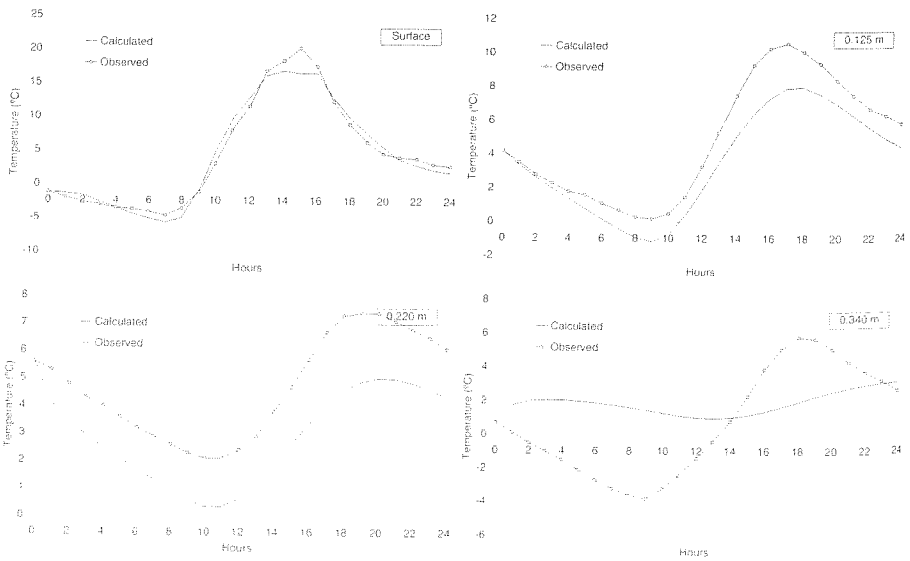

Figure 4. *Comparison between calculated and observed temperature for 2nd March*

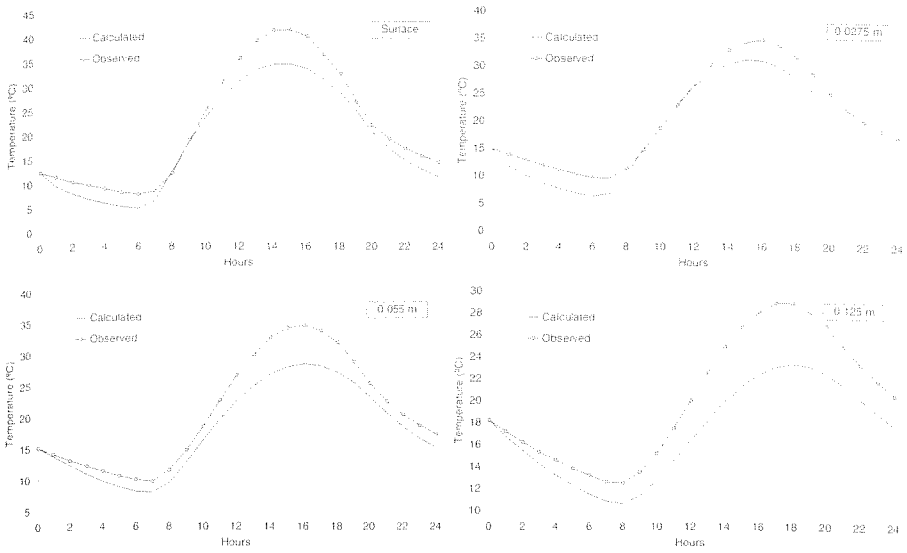

Figure 5. *Comparison between calculated and observed temperature for 24th April*

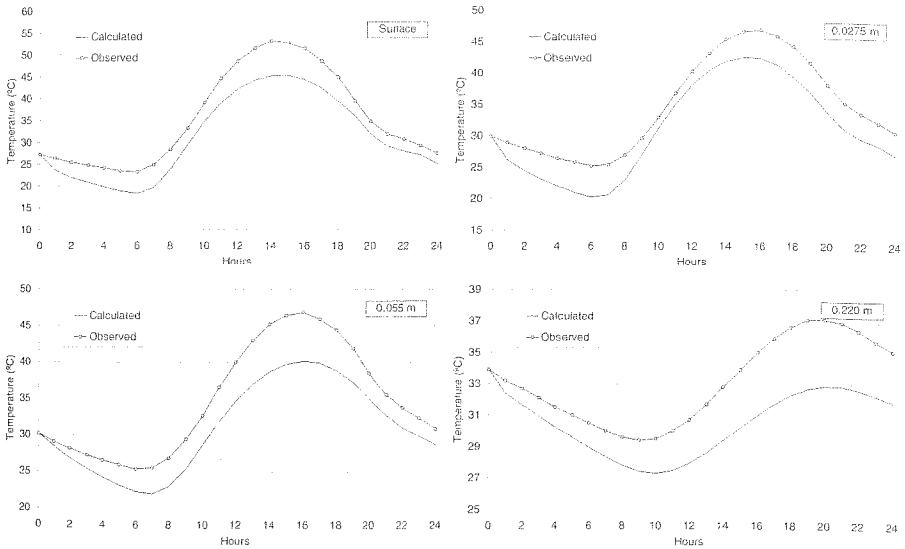

Figure 6. *Comparison between calculated and observed temperature for 24th July*

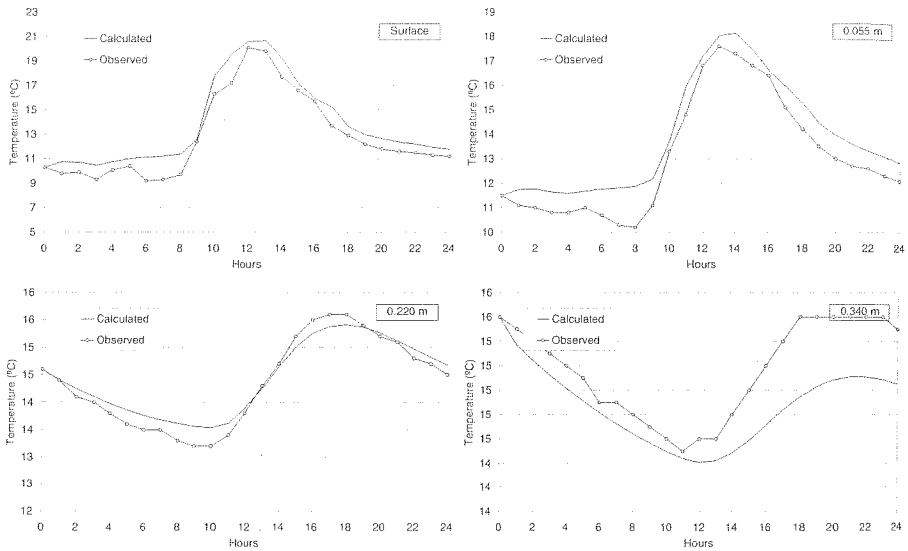

Figure 7. *Comparison between calculated and observed temperature for 16th October*

6. Conclusion

The 3-D finite-element analysis has proved to be an interesting tool to simulate the transient behaviour of asphalt concrete pavement temperature. According to comparisons performed with field measurements, the suggested simulation model can model the pavement temperature at different levels of bituminous layers with good accuracy. At close to the surface depths the measured and calculated temperatures presents better correlation than far to from the surface.

To obtain this distribution, a series of climatic data is needed as input to the model. The use of the results for other FEM mechanical models constitutes a great advantage of the proposed model.

When comparing measured and calculated temperature data for every hour for every day, one has concluded that in cold months, the average error is less than in hot months. Thus, in the cold months, the developed model presents better performance than in hot months.

The presence of an asphalt rubber mix layer in the top of the pavement seems to have no influence in the pavement temperature prediction and this type of material can be modelled with the specific heat and thermal conductivity coefficient identical to the ones used for conventional mixtures.

7. References

Sousa, Jorge B., Pais, Jorge C., Saim, Rachid, Way, George &, Stubstad, Richard N. "Development of a Mechanistic-Empirical Based Overlay Design Method for Reflective Cracking" *Transportation Research Record: Journal of the Transportation Research Record*, Nº 1809 - paper number 02-2846, TRB, National Research Council, Washington, D.C. 2002, pp 209-217.

de Bondt, Arian. "Effect of Reinforcement Properties". *Proceedings PRO11. 4th International RILEM Conference on Reflective Cracking in Pavements – Research in Practice*. Edited by A. O. Abd El Halim, D. S. A. Taylor and El H. H. Mohamed. RILEM. Ottawa, Ontario, Canada. March, 2000, pp 13-22.

A. Shalaby, Abd el Halim A.O and O.J. Svec. "Low-temperature stresses and fracture analysis of asphalt overlays". Proceedings. *Transportation Research Record: Journal of the Transportation Research Record*. Nº 1539, TRB, National Research Council. Washington, D.C. 1990. pp 132-139.

Donath M., Mrawira and Joseph Luca. "Thermal Properties and Transient Temperature Response of Full-Depth Asphalt Pavements". *Transportation Research Record: Journal of the Transportation Research Record*, Nº 1809 - paper number 02-4100, TRB, National Research Council. Washington, D.C. 2002, pp 160-169.

Dewit D. P. and F. P. Incopera. *Fundamentals of Heat and Mass transfer*. Edited by John Wiley and Sons. Toronto, Canada. 1996.

Ozisik M. N. *Heat Transfer: A Basic Approach*. Edited by McGraw-Hill. New York, USA. 1985.

Hermansson A., "A Mathematical Model for Calculating Pavement Temperatures, Comparisons between Calculated and Measured Temperatures". *Transportation Research Record: Journal of the Transportation Research Record*, Nº 1764 – paper number 01-3543. National Research Council. Washington, D.C., 2001.

Picado-Santos L., *Consideração da Temperatura no Dimensionamento de Pavimentos Rodoviários Flexíveis*. Ph. D. Tesis. University of Coimbra. Lisbon. 1994.

Minhoto, Manuel J.C., Pais, Jorge C., Pereira, Paulo A.A. & Picado-Santos, Luís G., "Low-Temperature Influence in the Predicted of Pavement Overlay", *Asphalt Rubber 2003 Conference*, Brasilia, Brasil, 2003, p. 167-180.

Minhoto, Manuel J. C., Pais, Jorge C., Pereira, Paulo A.A. & Picado-Santos, Luís G., "Predicting Asphalt Pavement Temperature with a Three-Dimensional Finite Element Model". *Transportation Research Record: Journal of the Transportation Research Board* nº 1919 – Rigid and Flexible Pavement Design 2005 – A peer reviewed publication. p. 96-110. TRB. Washington DC. 2005.